



# Cold Spring Harbor Symposia on Quantitative Biology

## A Physicist Looks at Bacterial Chemotaxis

H.C. Berg

*Cold Spring Harb Symp Quant Biol* 1988 53: 1-9

Access the most recent version at doi:[10.1101/SQB.1988.053.01.003](https://doi.org/10.1101/SQB.1988.053.01.003)

---

### References

This article cites 41 articles, 20 of which can be accessed free at:  
<http://symposium.cshlp.org/content/53/1.refs.html>

Article cited in:

<http://symposium.cshlp.org/content/53/1#related-urls>

### Email alerting service

Receive free email alerts when new articles cite this article - sign up in  
the box at the top right corner of the article or [click here](#)

---

---

To subscribe to *Cold Spring Harbor Symposia on Quantitative Biology* go to:  
<http://symposium.cshlp.org/subscriptions>

---

# A Physicist Looks at Bacterial Chemotaxis

H.C. BERG

Department of Cellular and Developmental Biology, Harvard University, Cambridge, Massachusetts 02138;  
Rowland Institute for Science, Cambridge, Massachusetts 02142

In this paper, a survey is given of the ways in which the enteric bacterium *Escherichia coli* (or *Salmonella typhimurium*) senses and responds to chemical stimuli. If one is to appreciate the molecular biology of signal transduction, it helps to understand the problems that the molecular biology is meant to solve. *E. coli* has managed to find its way in the world in the face of daunting physical constraints. These constraints arise because the organism is microscopic and immersed in an aqueous environment. In the realm of sensory transduction, not everything that is true for the colon bacillus is true for the elephant.

## Matters of Size

To better appreciate the subject of scale, consider the differences in size of *Homo sapiens*, *E. coli*, and the flagellar basal apparatus of *E. coli* (Fig. 1). *E. coli* lives in the human gut. It outnumbers all other motile organisms attending this Symposium by a very wide margin. It is remarkably small ( $10^{-4}$  cm in diameter, some

200,000 times smaller in diameter than *Homo sapiens*). It swims by rotating about six thin helical filaments (generally longer than those shown), which arise at random points on its surface. The motor that drives each filament is embedded in the cell wall and the cytoplasmic membrane and is smaller in diameter than the cell body by a factor of about 50.

## A Biased Random Walk

In the absence of a stimulus, *E. coli* simply wanders around, as illustrated in Figure 2. It swims smoothly by rotating its flagella counterclockwise (CCW). In this case, the filaments work together in a bundle that pushes the cell along a gently curved path, called a run. Runs are of random duration, distributed exponentially with a mean and standard deviation of about 1 second; the shortest runs are most probable. Runs are terminated by chaotic events, called tumbles, that arise when the flagella rotate clockwise (CW). In this event, the filaments work independently, moving the cell errati-

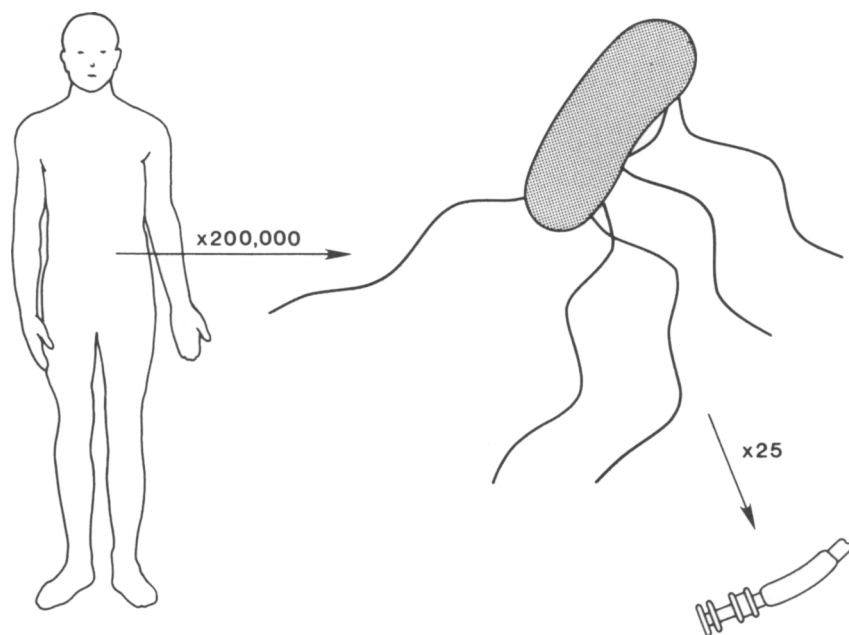


**Figure 1.** Comparison of the size of man, *E. coli*, and part of *E. coli*'s flagellar motor. The flagellar motor is some five million times smaller in diameter than one's fist. The sources of the diagrams are as follows: Man is adapted from Fig. 144 of Gray (1954). The bacterium is a tracing of Fig. 1 of Adler (1965), the publication that heralded modern work on bacterial chemotaxis. The motor fragment is a schematic outline of Fig. 1a of DePamphilis and Adler (1971), which showed the proximal end of a flagellum extracted from a cell by a neutral detergent and negatively stained with uranyl acetate. The curved segment is the proximal hook, which is on the outside of the cell. The adjacent pair of rings is a bushing that gets the drive shaft through the outer cell membrane. The inner pair of rings comprise part of the rotor and stator. The innermost ring is embedded in the cytoplasmic membrane.

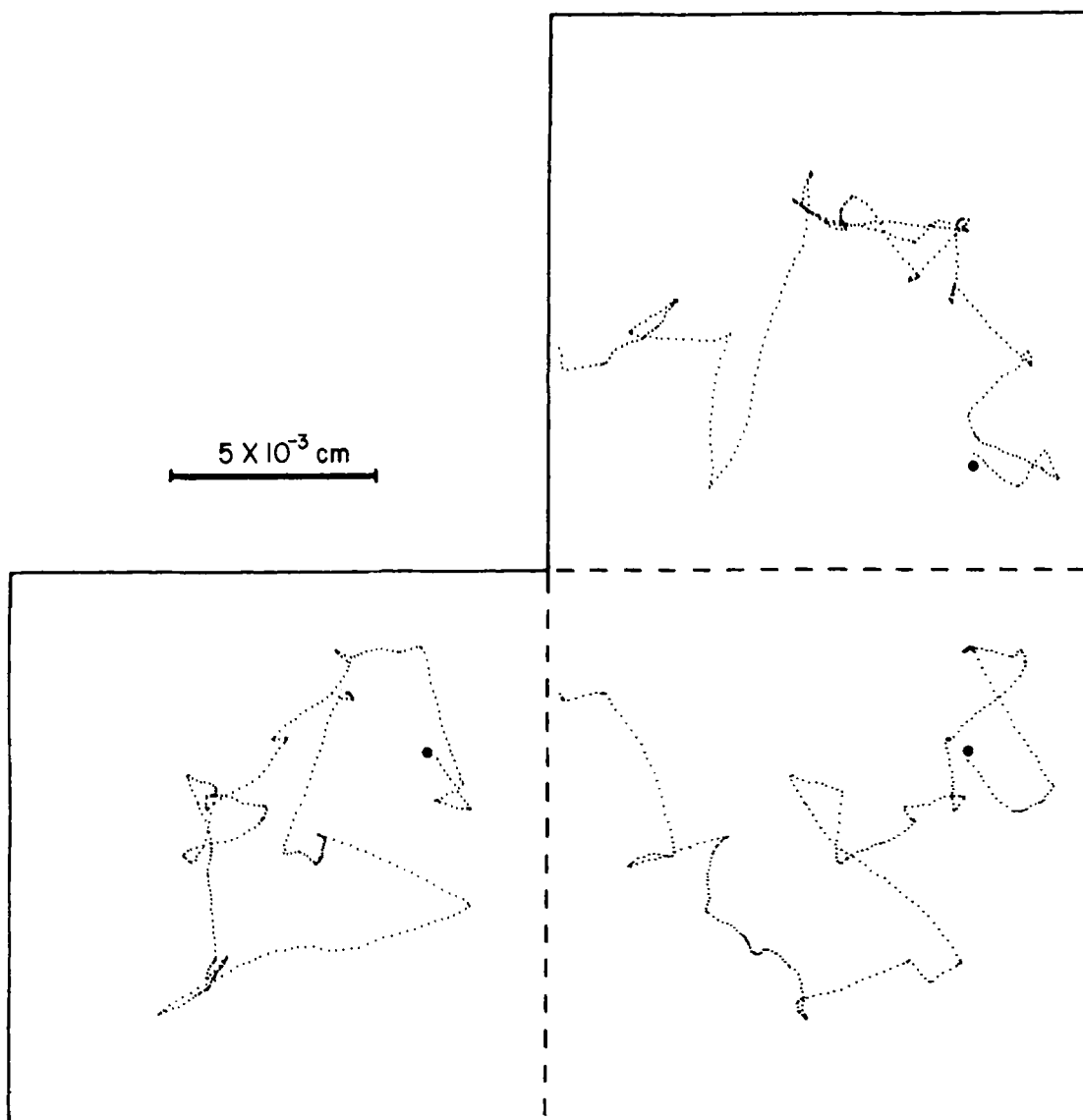


**Figure 2.** A digital plot (12.6 points/sec) of the displacement of a wild-type cell (*E. coli* strain AW405) executing a random walk in a homogeneous, isotropic medium. These are planar projections of a three-dimensional track: If the left and upper panels are folded out of the page along the dotted lines, the projections appear in proper orientation on three adjacent faces of the cube. Tracking began at the large dot and continued for about 30 sec. The cell swam at the speed of  $\sim 2 \times 10^{-3}$  cm/sec. There were 26 runs and tumbles. (Reprinted, with permission, from Fig. 6.4 of Berg 1983, which was based on Fig. 1 of Berg and Brown 1972.)

cally with little net displacement. Tumbles also are of random duration, distributed exponentially, with a mean and standard deviation of about 0.1 second. Following a tumble, the cell runs again, picking a new direction, more or less at random. When the cell swims in a spatial gradient of a chemical attractant, runs that happen to carry it up the gradient are extended, whereas those that happen to carry it down the gradient are not. Thus, the cell drifts in a favorable direction by executing a biased random walk. The bias is positive, not negative; the runs get longer, not shorter. *E. coli* is an "optimist."

#### Limits Set by Physics

Physical constraints influence this sensory strategy in several ways: (1) The flagellar filaments are long, thin,

and helical because motion is dominated by viscous rather than inertial forces. It sounds contradictory, but thrust must be generated by viscous drag. (2) A cell is unable to run in a straight line, because rotational perturbations due to Brownian movement knock it off its path. *E. coli* forgets where it is going in about 10 seconds. (3) A cell cannot improve its lot locally by swimming or stirring, because transport of small molecules is effected by diffusion rather than bulk flow. Local displacements of the fluid do not increase the cell's nutritional intake. (4) A cell must sense a chemical gradient temporally rather than spatially, because comparisons between concentrations in front or behind are overwhelmed by diffusive currents due to its rapid motion. Although the net increase in intake is very small, a cell always absorbs more molecules in front than behind. Therefore, with a spatial mechanism, any

new direction is deemed favorable. Finally, (5) the precision with which a cell can make temporal comparisons is limited by statistical fluctuations. The counting statistics improve with the square root of the product of the concentration and the integration time. Therefore, a chemical cannot be sensed at an arbitrarily low concentration, because the integration time required would be prohibitively long. For further discussion, see Berg and Purcell (1977), or for treatments that are less mathematical, see Purcell (1977) and Berg (1985).

### Mapping Responses in Time and Space

The time scale on which *E. coli* measures changes in its environment and the spatial scale on which signals are propagated internally from the chemoreceptors to the flagella have been determined by delivering chemical attractants (e.g., aspartate) or repellents (e.g., benzoate) with iontophoretic pipettes, as shown in Figure 3. In panel a, a cell is tethered to a glass surface by the stub of a single flagellar filament (following mechanical shear and the addition of antifilament antibody; cf. Silverman and Simon 1974). In panel b, an inert marker (a cell with abnormally long proximal hooks, called polyhooks, killed by fixation with glutaraldehyde) is attached to a polyhook of a living filamentous cell (by addition of antihook antibody; cf. Ishihara et al. 1983). The tethered cell or the inert marker spin alternately CW or CCW, reversing their directions at random times, on average about once per second. In a strain that is wild type for chemotaxis, the fraction of time that the cell or marker spins CCW (called the bias) is roughly one-half. Control of the addition of the attractant or repellent can be effected with a precision of a few milliseconds by passing a current through the pipette. In Figure 3a, the tip of the pipette is fixed a few

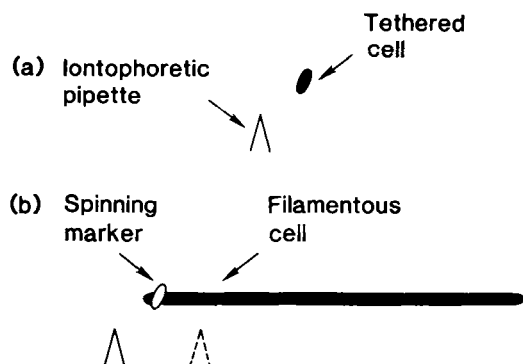


**Figure 3.** A schematic illustration of experiments in which a tethered cell (a) or a filamentous cell (b) is simulated by ejection of a charged chemical from the tip of an iontophoretic pipette. (a) The pipette is fixed; (b) it is moved to a series of alternative positions, one of which is shown (dashed inverted "V"). The tethered cell is driven by one of its own flagellar motors. The marker is inert, but it spins because it is linked to one of the motors of the filamentous cell. Filamentous cells can be prepared from nonseptate mutants or by growing ordinary cells in the presence of a  $\beta$ -lactam antibiotic (see Block et al. 1982; Ishihara et al. 1983; Segall et al. 1985).

micrometers away from the tethering axis. In Figure 3b, it is moved through a series of positions off the end of the filamentous cell or along the cell body (at similar distances from the marker, as shown by the dashed inverted "V").

### Impulse Responses

When the experiment of Figure 3a is done with short impulsive stimuli (e.g., with pulses of aspartate of small amplitude and width), a biphasic response is obtained, as shown in Figure 4. The bias rises rapidly, returns to the baseline after about 1 second, falls below the baseline, and then returns to the baseline again after another 3 seconds; the areas of the positive and negative lobes are the same. If one uses a pulse of similar width but smaller amplitude, the response follows the same time course; only its amplitude is smaller. Evidently, a transient increase in occupancy of the aspartate receptor sets in motion a train of events that affect the direction of rotation of the flagellar motor for a span of 4 seconds. If one uses a mutant deleted for the genes *cheR* and *cheB*, whose products are enzymes that carboxymethylate and demethylate the receptor, respectively (see below), the second lobe of the response is missing. If one uses an amber mutant of *cheZ*, whose wild-type product is another cytoplasmic protein, the whole process slows down by a factor of about 10 (cf. Segall et al. 1986).

### What *E. coli* Measures

Given a linear system, e.g., one without thresholds that is exposed to small stimuli, one can use the impulse response (Fig. 4) to predict the behavior expected with any stimulus. The impulse response is a weighting function, in the following sense. To discover how the pres-

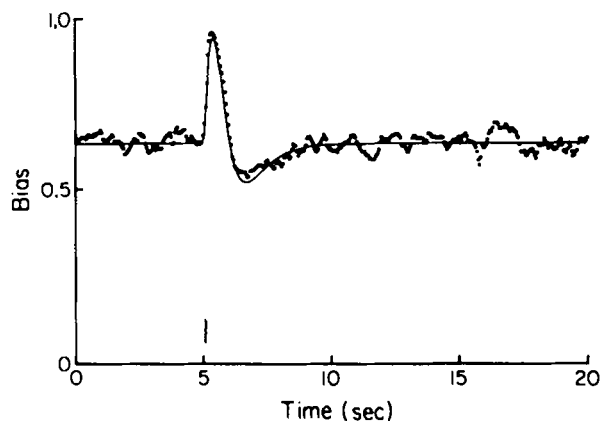


**Figure 4.** The response of tethered wild-type cells to a pulse of attractant (aspartate or  $\alpha$ -methylaspartate) delivered iontophoretically (at time 5.06 sec, vertical bar). The dotted curve is the probability of CCW rotation (the bias) determined for wild-type strain AW405 by repetitive stimulation. The smooth curve is a fit to a sum of exponentials. The stimuli were equivalent to a pulse that increases the receptor occupancy by 0.19 for a period of 0.02 sec (the shortest pulse used in the experiments). (Reprinted, with permission, from Fig. 1 of Segall et al. 1986.)

ent bias of a cell deviates from its baseline, proceed as follows: (1) Plot the concentration of the attractant for the past several seconds on the same time scale as that in Figure 4, setting the present time at the vertical bar but going backwards in time from left to right. (2) Multiply the two curves together, calling the baseline of the impulse response zero. (3) Integrate to find the area of the product. The shift in bias is proportional to this number. Because the impulse response (for the wild type) remains at its baseline (the zero value) for times greater than 4 seconds, the present bias depends only on events that have occurred during the past 4 seconds. Because the areas of the two lobes of the impulse response are the same, a shift in bias will occur only if the concentration has changed over that time. In brief, wild-type cells exposed to stimuli in the physiological range make short-term temporal comparisons extending 4 seconds into the past: the past 1 second is given a positive weighting, the previous 3 seconds are given a negative weighting, and the cells respond to the difference.

The impulse response for repellent stimuli is similar to that for attractant stimuli (Fig. 4) but inverted (cf. Fig. 3 in Block et al. 1982). However, experiments in which the concentrations of attractants or repellents are varied over long periods of time by programmed mixing indicate that repellent stimuli are subject to a substantial threshold. Beyond a certain point, cells simply ignore gradual increases in the concentrations of repellents (or gradual decreases in the concentrations of attractants) (see Block et al. 1983). This mechanism underlies *E. coli*'s optimism.

### Temporal Sensing

These temporal comparisons are made continuously, regardless of whether the cells run or tumble. This was evident early on from experiments in which an attractant (glutamate) was generated or destroyed enzymatically (by the action of alanine aminotransferase) in a solution containing swimming cells (of a mutant insensitive to alanine) that was otherwise homogeneous and isotropic (Brown and Berg 1974). When the attractant was generated, the cells swam in a random fashion, as before (i.e., as in Fig. 2), but all the runs were longer, regardless of the direction in which a cell happened to swim. When the attractant was destroyed (at a rate below the threshold noted above), no changes in behavior were observed.

The changes in bias found in experiments with programmed mixing are directly proportional to the time rate of change in receptor occupancy (Block et al. 1983). As noted by Delbrück and Reichardt (1956), comparisons between the recent and more distant past require at least two biochemical processes, one that occurs rapidly (e.g., within 1 sec of the specified change in receptor occupancy) and the other more slowly (e.g., during the following 3 sec). We know relatively little about the rapid process (or processes). The slow pro-

cess, as we have seen from the disappearance of the second lobe of the impulse response in *cheR cheB* mutants, involves receptor carboxymethylation.

### Saturation of the Response

It has proved convenient to separate rapid from slow changes that occur during signal processing by exposing cells suddenly to large changes in the concentrations of attractants or repellents. In this event, the response saturates rapidly (the bias goes to 1 or to 0 within about 0.2 sec; cf. Segall et al. 1982), and it remains saturated for a very long time (up to several min). The interval required for the bias to saturate has been called an "excitation time," and the interval required for the bias to come back on scale has been called a "recovery time" (Spudich and Koshland 1975) or a "transition time" (Berg and Tedesco 1975). But note that these excitation, or recovery, times are not related in any simple way to the times that characterize signal processing of stimuli in the normal physiological range. Cells swimming in the wild never see such abrupt and large temporal stimuli, because discontinuities in concentration are smoothed out by diffusion. Cells are sensitive to gradients only when the bias is on scale.

### Gain of the System

The gain of the signal-processing system is prodigious. A step change that increases the occupancy of the aspartate receptor by 1 molecule (assuming 600 receptor molecules per cell) increases the rotational bias transiently by about 0.1. A ramp that increases the receptor occupancy by one molecule per second leads to a steady-state increase in bias of a similar magnitude.

### An Optimum Strategy

The impulse response (Fig. 4) is matched to the random walk (Fig. 2). In trying to decide whether life is getting "better" or "worse," the cell averages concentrations for as long as it can ( $\sim 1$  sec). It does this to avoid being overwhelmed by fluctuations. However, if this integration time were much longer than 1 second, several tumbles could occur before a decision were reached, and the results would no longer be relevant. Note that the cell cannot solve this problem by making the mean run length longer, because rotational Brownian movement carries it off course by as much as  $90^\circ$  within 10 seconds. The cell sets the mean run length at 1 second to provide ample head room for a response, and it extends runs rather than shortening them to minimize changes in direction that might occur during the integration time.

### A Simulation

One can put all of this together in a simulation of the sort shown in Figure 5. The slide used at the Sym-

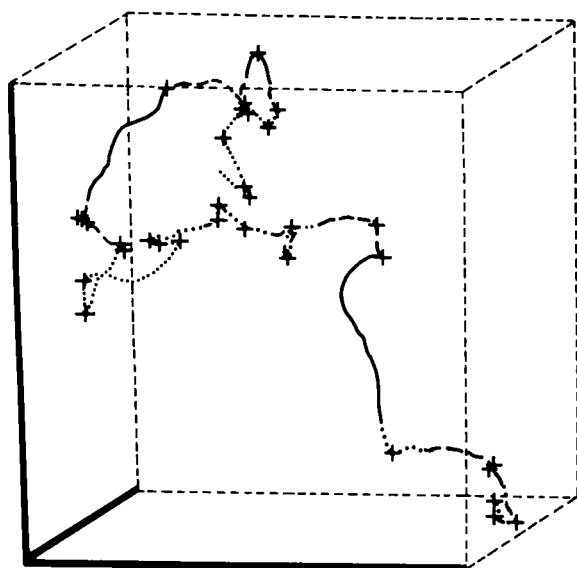


**Figure 5.** Simulation of the behavior of a wild-type cell in an exponential gradient of attractant (aligned in the vertical direction, positive upward, corresponding to an increment in receptor occupancy of 1 part in  $10^4/\mu\text{m}$  at a mean occupancy of 0.5). The coordinate axes are  $\sim 200 \mu\text{m}$  long. The cell started off in a direction chosen at random near the bottom right edge of the figure. It ran at a fixed speed of  $20 \mu\text{m}/\text{sec}$ . There were 35 runs and 34 tumbles. The value of the internal parameter setting the probability of a tumble is indicated by the nature of the line: large (dotted here; blue in the original), medium (dashed; yellow), small (solid; red). Other details are given in the text. (Figure courtesy of S.M. Block.)

posium was in color, which was more dramatic. The color (mimicked here by dots, dashes, and solid lines) indicates the value of an internal parameter that one might call "happiness," the signal that sets the bias, i.e., that determines the probability that the cell runs or tumbles. This parameter is computed by using the impulse response (Fig. 4) to weight the recent and more distant past in the manner described earlier. If the cell is running and the output of this computation (called a convolution) is negative, i.e., if the concentration has been decreasing for some time, the result is ignored, and the cell decides whether it should tumble by picking from an exponential distribution with a mean of 1 second. If the cell is running and the output of the convolution is positive, the cell picks from an exponential distribution with a larger mean (one with an exponent decreased in linear proportion to that output). On the other hand, if the cell is tumbling, it decides whether it should run by picking from an exponential distribution with a mean of 0.1 second. If a new run is called for, the cell heads in a direction that differs from that at the end of the previous run by a random choice from a distribution of angles peaked somewhat in the forward direction (cf. Fig. 3 in Berg and Brown 1972). Brownian rotation is included by giving the cell a small kick in angle every iteration (every 0.01 sec). For the simulation shown here, the gain of the system was chosen to be optimum, i.e., so that the probability of terminating a run would just go to zero if a cell were to

swim unerringly straight up the gradient. Simulations of 100 cells for 10 minutes each gave a mean draft rate of  $1.7 \mu\text{m}$  per second ( $\sim 8\%$  of the run speed).

When watching such tracks evolve on a computer screen, one gets the impression of a bloodhound following a scent. The cell sniffs about (dotted or blue), picks up the spoor (dashed or yellow), and then howls up the gradient (solid or red). Eventually, rotational Brownian motion carries it off the track, and it is forced to sniff about again. Note that for this cell (Fig. 5), most of the progress up the gradient occurred in two long runs (solid lines). The reason for playing this game is more serious than reference to bloodhounds might suggest. First, we would like to know whether we really understand the behavior of wild-type cells. Second, we would like to predict, from measurements of impulse responses of tethered chemotactic mutants, how pathological their swimming behavior might be.

### Biochemistry and Genetics

What is the machinery that enables a creature of such small size to manage such remarkable sensory feats? The biochemical landscape is sketched in Figure 6. For more information, see the recent and extensive reviews of Stewart and Dahlquist (1987) and Macnab (1987a,b). Three major systems for chemoreception have been recognized. The first, noted at the top of Figure 6, detects serine and certain repellents such as leucine (mediated by Tsr = MCPI [methyl-accepting chemotaxis protein I]), aspartate and certain other repellents such as  $\text{Ni}^+$  (mediated by Tar = MCP II), dipeptides (mediated by Tap), and ribose and galactose (mediated by Trg = MCPIII). The second, shown at the left, detects sugars transported by the sugar phosphotransferase system. The third, shown at the bottom, detects oxygen and certain other electron acceptors. The first of these systems has been studied most extensively. For literature on the second and third systems, see Macnab (1987b), Vogler and Lengeler (1987), and Shioi et al. (1987). The chemotaxis genetic map is shown in Figure 7.

### Transporting Information Across the Cytoplasmic Membrane

The proteins Tsr, Tar, Tap, and Trg bind ligands either directly or indirectly and mediate responses for several different kinds of inputs; therefore, they have been called transducers. Their genes appear to be members of one family, and they are composed of discrete structural and functional domains (cf. Krikos et al. 1983; Bollinger et al. 1984). The periplasmic domains are divergent, whereas the cytoplasmic domains are highly conserved. The former contain binding sites for attractants or attractant-binding proteins, whereas the latter contain two sets of clustered sites for methylation and a region thought to be involved in relaying the signal to the flagella. One transducer, the Tar protein, is shown schematically in Figure 8. An

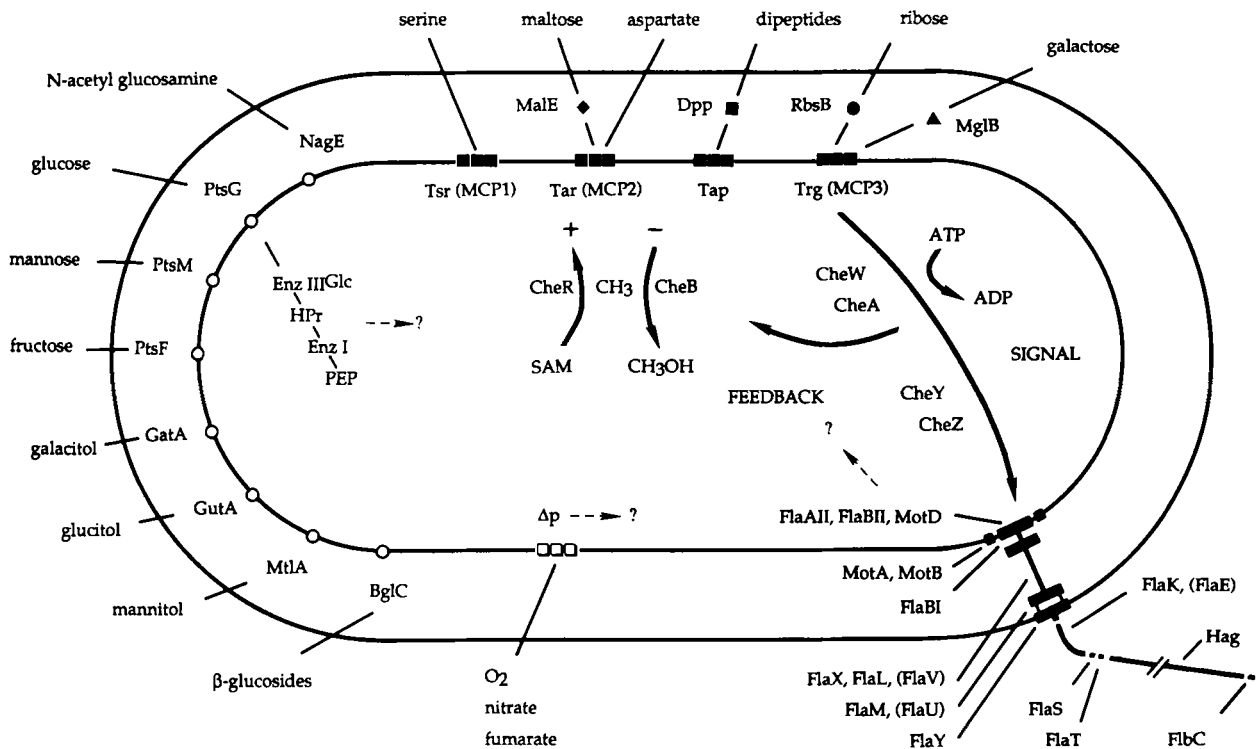


**Figure 6.** Machinery for chemotaxis in *E. coli* that has been identified thus far. The chemoreceptors are binding proteins found in the periplasmic space, such as MalE (which binds maltose), or proteins that span the cytoplasmic membrane, such as Tsr (which binds serine) or the enzymes II of the sugar phosphotransferase system, such as MtlA (which binds mannitol). Information about receptor occupancy is passed across the cytoplasmic membrane and eventually to the base of the flagellar motors, where it changes the probabilities that the motors turn CW or CCW. This signalling occurs through a cascade of events involving the cytoplasmic proteins CheW, CheA, CheY, and CheZ. A negative feedback loop counteracts the effects of this signal, enabling the cells to adapt. In the system studied most extensively, which involves the transducers Tsr, Tar, Tap, and Trg (also called MCPs), this feedback is effected by carboxymethylation of cytoplasmic domains. When more attractant is bound, methyl groups ( $\text{CH}_3$ ) are transferred from *S*-adenosylmethionine (SAM) via a methyltransferase (CheR). When less attractant is bound, these methyl groups are removed by a methyl-erasure (CheB), liberating methanol ( $\text{CH}_3\text{OH}$ ). In the Pts and  $\text{O}_2$  systems, the signal and feedback pathways are not known, although signaling in the latter system might involve changes in protonmotive force ( $\Delta p$ ). Components of the flagellar motor, hook, and filament are shown at the lower right. Fla components are required for flagellar assembly. FlaAII and FlaBII comprise the switch that enables a motor to change direction. The gene products shown in parentheses are not structural components per se but are required for proper assembly, e.g., FlaE controls the length of the hook (FlaK). Hag is the structural protein of the filament (flagellin). FlaS, FlaT, and FlbC are the so-called hook-associated proteins. MotA and MotB are required for force generation.

unanswered question, relevant to many other receptor systems, is how sensory information moves from the periplasmic domain to the cytoplasmic domain.

### Linking the Transducers to the Flagella

The information-processing pathway is convergent. Information flows from many receptor molecules of several different kinds to a few flagellar motors (Fig. 6). Measurements of external concentration can be made most effectively (integration times can be shortened) if these receptors are scattered widely over the surface of the cell and if each contributes its bit to the signal that controls the direction of flagellar rotation (Berg and Purcell 1977). How is this coupling achieved? One approach to answering this question is illustrated in Figure 3b. When the pipette was close to the cell surface (as indicated by the dashed inverted "V"), the response of the motor driving the marker was larger than when the pipette was off the end of the

cell (as indicated by the solid inverted "V"). This would be expected if there were an internal signal, because more receptors are influenced by the pipette when it is close to the cell surface. However, this effect faded rapidly as the pipette was moved farther away (beyond a few microns), indicating that the range of the internal signal is short. These data ruled out a number of possible mechanisms, including those involving changes in membrane potential (see also Margolin and Eisenbach 1984). Mutants of *cheZ* yielded a range longer by a factor of about 3. This inspired a hypothesis in which a small protein, CheY, is activated at the receptors and inactivated by CheZ as it diffuses through the cytoplasm. Active CheY binds to the components of the flagellar switch and enhances CW rotation.

CheY has been shown to have just such an effect (Clegg and Koshland 1984; Ravid et al. 1986; Wolfe et al. 1987). Indeed, the coupling pathway for a response to aspartate can be restored by adding back the compo-

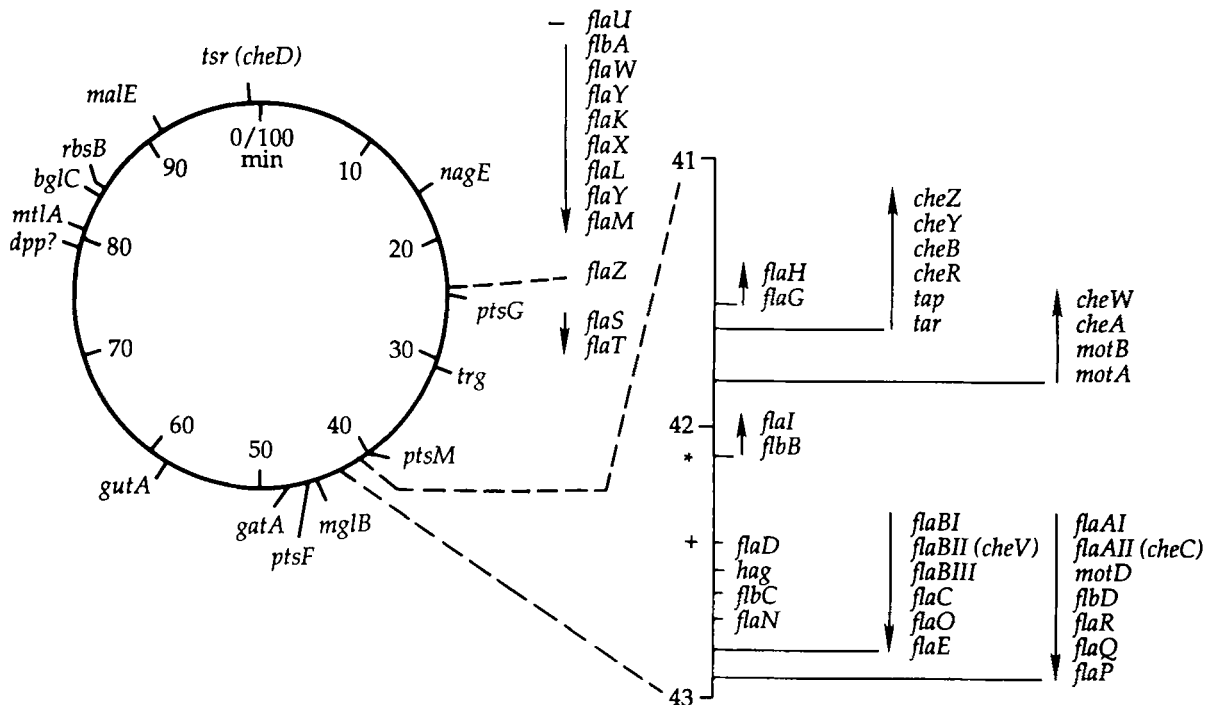


**Figure 7.** Genetic map of chemotaxis loci in *E. coli*. The numbers indicate map position in minutes. The arrows indicate the direction and extent of transcriptional units. (\*) Master operon, turned on by cAMP and a catabolite activator protein (cap); (+) positive regulator of late operons; (−) negative regulator of late operons; late operons include hook-associated proteins (FlaS, FlaT, FlbV), Mot, Che, Hag (via FlaZ). The only *pts* genes shown are those for EnzII. Genes required for appearance of first incomplete flagellum structure: *flbA*, *flaW*, *flaX*, *flaL*; *flaZ*; *flaG*, *flaH*; *flbB*, *flaI*; *flaD*; *flaN*; *flaBI*, *flaBII*, *flaBIII*, *flaC*, *flaO*, *flaAI*, *flaAII*, *motB*, *flbD*, *flaR*, *flaW*, *flaP*. (Adapted from Fig. 1 of Parkinson [1981], using data tabulated by Macnab [1987b].)

nents Tar, CheW, CheA, and CheY to a cell that has been "guttled" for all of the transducers (Tsr, Tar, Tap, and Trg) and all of the soluble *che* gene products (CheW, CheA, CheR, CheB, CheY, and CheZ; Wolfe et al. 1987). Both CheW and CheA appear to be required (A.J. Wolfe et al., in prep.).

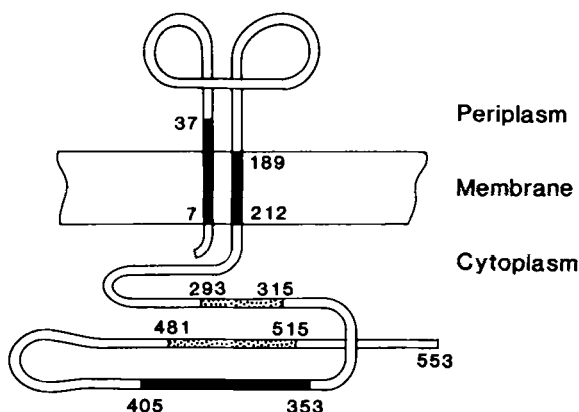


**Figure 8.** A schematic representation of the transducer Tar. The numbers refer to the positions of the amino acids in the peptide chain (shown as a ribbon), beginning at the amino terminus. Methylation of glutamyl residues occurs in two regions, between amino acids 293 and 315 (called  $K_1$ ) and 481 and 515 (called  $R_1$ ). The region between amino acids 405 and 353 is identical in Tsr, Tar, Tap, and Trg and is thought to be involved in signaling (cf. Mutoh et al. 1986). (Adapted from Fig. 6 of Krikos et al. [1983] and Fig. 5 of Russo and Koshland [1983].)

## Phosphorylation

This discussion has been enriched enormously by the recent in vitro findings of Simon and co-workers (reviewed by Parkinson 1988) that CheA autophosphorylates (Hess et al. 1987), that phosphorylated CheA, in turn, phosphorylates CheY and CheB (Hess et al. 1988), and that CheZ accelerates the dephosphorylation of CheY (Hess et al. 1988). In addition, mutants of *cheA* defective in chemotaxis are defective in phosphorylation (Oosawa et al. 1988). Work of a similar nature on CheA and CheY has been reported by Stock et al. (1988) and Wylie et al. (1988). Thus, it appears that information transfer occurs via a cascade of reactions involving protein phosphorylation.

## Other Modifications

In pursuing work on gutted cells containing CheY, A.J. Wolfe and M.P. Conley stumbled onto a surprising effect in which acetate but not benzoate enhances CW rotation. Normally, weak acids act by lowering the cytoplasmic pH, which perturbs both Tsr (leading to a CW response) and Tar (leading to a CCW response); benzoate is more effective than acetate. The acetate effect in gutted cells containing CheY has been traced to the intermediate acetyladenylylate and the enzyme acetate-CoA synthetase. Mutants defective in the latter enzyme, which grow if given oleic acid, fail to respond in capillary assays to serine, aspartate, or maltose.



Therefore, it is possible that phosphorylation will not be the only modification: Other kinds of chemical modification, such as acetylation or adenylation, might occur at other stages in the signaling pathway (Wolfe et al. 1988).

### Feedback

A branch in the pathway generating negative feedback via CheB occurs between CheA and CheY (Fig. 6). This branch has been studied extensively by Dahlquist and his co-workers, who have labeled cells with radioactive methionine and followed the evolution of radioactive methanol (cf. Kehry et al. 1985; Stewart and Dahlquist 1987). Because chemotaxis cannot occur if the rotational basis is 0 or 1, one also would expect feedback at the level of the flagellar motor (indicated by the dashed arrow and question mark in Fig. 6), but this branch remains to be identified.

### Stochastic Output

What does the signal do when it reaches the flagellar motors? Experiments with filamentous cells carrying multiple markers (Ishihara et al. 1983) or with cells of normal size viewed with high-intensity light (Macnab and Han 1983) indicate that the motors do not change direction synchronously. The signal determines the rates at which transitions occur between CW and CCW states, not the transition times per se. Our current thinking is that activated CheY binds to FlaAII and/or FlaBII, changing these rates, and that CheY, once bound, is sensitive to attack by CheZ. But this is probably naive, because so little is known about how the motor controls its direction of rotation. Evidently, the coordination required for formation of a flagellar bundle arises from external interactions between different flagellar filaments.

### The Rotary Motor

The flagellar motor is a remarkable machine. For one suggestion as to how it might work, see Berg and Khan (1983) or Khan and Berg (1983). Its specifications are given in Table 1. The speed is the value recorded in swimming cells at room temperature (Lowe et al. 1987). The power output seems miniscule, until one divides by the weight; internal combustion engines do no better (cf. McMahon and Bonner 1983). The motor is driven by an inward flux of protons (or hydronium ions); about 1000 are required per revolution (Meister et al. 1987). Proceeding more systematically than possible in earlier work (Block and Berg 1984), D.F. Blair has induced the synthesis of wild-type MotA and/or MotB in *mot<sup>-</sup>* strains of *E. coli* and found several examples in which tethered cells reach their top speed in eight steps; therefore, we now believe that there are only eight independent force-generating units (D.F. Blair and H.C. Berg, in prep.). For more information

**Table 1. Motor Specifications (Approximate)**

Feature	Specifications
Diameter	1 micro inch
Speed	6000 rpm
Power output	1/10 micro micro hp
Power output per unit weight	10 hp per pound
Power source	proton current
Cylinders	8
Number of different kinds of parts	30
Gears	forward and reverse

about motor components, see Macnab (this volume). It is the gears that are critical for chemotaxis.

### SUMMARY

What is distinctive about bacterial chemotaxis, as compared to, for example, taste in the elephant, is the time over which decisions must be made. The lower limit is set by diffusion of chemicals to and from the cell surface, which demands long times for statistically significant counts. The upper limit is set by diffusion of the cell itself, which demands short times for well-defined swimming paths. For an organism the size of *E. coli*, temporal comparisons of the concentrations of chemicals in the environment must be made within a few seconds. Although such short time spans might be difficult for the biochemist, they are not so difficult for *E. coli*, because diffusion can carry a small molecule across the cell in about 1 msec. *E. coli* has the opposite problem: How does it integrate inputs from many receptors over periods 1000 times as long?

The mechanisms for this signal processing are beginning to be understood. We know how most chemical attractants are identified, how temporal comparisons might be made, and how the behavioral output is effected. We know less about how sensory information crosses the cytoplasmic membrane, how the reactions that link the receptors to the flagella generate such high gain, and what actually controls the direction of flagellar rotation.

One thing is quite clear: *E. coli* demands our admiration and respect.

### ACKNOWLEDGMENTS

I thank Karen Fahrner for her comments on the manuscript. This work was supported by grants from the National Science Foundation (DMB-8518257) and the National Institute of Allergy and Infectious Diseases (AI-16478).

### REFERENCES

- Adler, J. 1966. Chemotaxis in *Escherichia coli*. *Cold Spring Harbor Symp. Quant. Biol.* **30**: 289.  
 Berg, H.C. 1983. *Random walks in biology*. Princeton University Press, Princeton, New Jersey.

- . 1985. Physics of bacterial chemotaxis. In *Sensory perception and transduction in aeneural organisms* (ed. G. Colombetti et al.), p. 19. Plenum Press, New York.
- Berg, H.C. and D.A. Brown. 1972. Chemotaxis in *Escherichia coli* analysed by three-dimensional tracking. *Nature* **239**: 500.
- Berg, H.C. and S. Khan. 1983. A model for the flagellar rotary motor. In *Mobility and recognition in cell biology* (ed. H. Sund and C. Veeger), p. 485. Walter de Gruyter, Berlin.
- Berg, H.C. and E.M. Purcell. 1977. Physics of chemoreception. *Biophys. J.* **20**: 193.
- Berg, H.C. and P.M. Tedesco. 1975. Transient response to chemotactic stimuli in *Escherichia coli*. *Proc. Natl. Acad. Sci.* **72**: 3235.
- Block, S.M. and H.C. Berg. 1984. Successive incorporation of force-generating units in the bacterial rotary motor. *Nature* **309**: 470.
- Block, S.M., J.E. Segall, and H.C. Berg. 1982. Impulse responses in bacterial chemotaxis. *Cell* **31**: 215.
- . 1983. Adaptation kinetics in bacterial chemotaxis. *J. Bacteriol.* **154**: 312.
- Bollinger, J., C. Park, S. Harayama, and G.L. Hazelbauer. 1984. Structure of the Trg protein: Homologies with and differences from other sensory transducers of *Escherichia coli*. *Proc. Natl. Acad. Sci.* **81**: 3287.
- Brown, D.A. and H.C. Berg. 1974. Temporal stimulation of chemotaxis in *Escherichia coli*. *Proc. Natl. Acad. Sci.* **71**: 1388.
- Clegg, D.O. and D.E. Koshland, Jr. 1984. The role of a signaling protein in bacterial sensing: Behavioral effects of increased gene expression. *Proc. Natl. Acad. Sci.* **81**: 5056.
- Delbrück, M. and W. Reichardt. 1956. System analysis for the light growth reactions of *Phycomyces*. In *Cellular mechanisms in differentiation and growth* (ed. D. Rudnick), p. 3. Princeton University Press, Princeton, New Jersey.
- DePamphilis, M.L. and J. Adler. 1971. Fine structure and isolation of the hook-basal body complex in flagella from *Escherichia coli* and *Bacillus subtilis*. *J. Bacteriol.* **105**: 384.
- Gray, H. 1954. *Anatomy of the human body*, 26th ed. (ed. C.M. Goss), p. 135. Lea and Febiger, Philadelphia, Pennsylvania.
- Hess, J.F., K. Oosawa, N. Kaplan, and M.I. Simon. 1988. Phosphorylation of three proteins in the signaling pathway of bacterial chemotaxis. *Cell* **53**: 79.
- Hess, J.F., K. Oosawa, P. Matsumura, and M.I. Simon. 1987. Protein phosphorylation is involved in bacterial chemotaxis. *Proc. Natl. Acad. Sci.* **84**: 7609.
- Ishihara, A., J.E. Segall, S.M. Block, and H.C. Berg. 1983. Coordination of flagella on filamentous cells of *Escherichia coli*. *J. Bacteriol.* **155**: 228.
- Kehry, M.R., T.G. Doak, and F.W. Dahlquist. 1985. Sensory adaptation in bacterial chemotaxis: Regulation of demethylation. *J. Bacteriol.* **163**: 983.
- Khan, S. and H.C. Berg. 1983. Isotope and thermal effects in chemiosmotic coupling to the flagellar motor of *Streptococcus*. *Cell* **32**: 913.
- Krikos, A., N. Mutoh, A. Boyd, and M.I. Simon. 1983. Sensory transducers of *E. coli* are composed of discrete structural and functional domains. *Cell* **33**: 615.
- Lowe, G., M. Meister, and H.C. Berg. 1987. Rapid rotation of flagellar bundles in swimming bacteria. *Nature* **325**: 637.
- Macnab, R.M. 1987a. Flagella. In *Escherichia coli and Salmonella typhimurium: Cellular and molecular biology* (ed. F.C. Neidhardt et al.), vol. 1, p. 70. American Society for Microbiology, Washington, D.C.
- . 1987b. Motility and chemotaxis. In *Escherichia coli and Salmonella typhimurium: Cellular and molecular biology* (ed. F.C. Neidhardt et al.), vol. 1, p. 732. American Society for Microbiology, Washington, D.C.
- Macnab, R.M. and D.P. Han. 1983. Asynchronous switching of flagellar motors on a single bacterial cell. *Cell* **32**: 109.
- Margolin, Y. and M. Eisenbach. 1984. Voltage clamp effects on bacterial chemotaxis. *J. Bacteriol.* **159**: 605.
- McMahon, T.A. and J.T. Bonner. 1983. *On size and life*, p. 60. Scientific American Books, New York.
- Meister, M., G. Lowe, and H.C. Berg. 1987. The proton flux through the bacterial flagellar motor. *Cell* **49**: 643.
- Mutoh, N., K. Oosawa, and M.I. Simon. 1986. Characterization of *Escherichia coli* chemotaxis receptor mutants with null phenotypes. *J. Bacteriol.* **167**: 992.
- Oosawa, K., J.F. Hess, and M.I. Simon. 1988. Mutants defective in bacterial chemotaxis show modified protein phosphorylation. *Cell* **53**: 89.
- Parkinson, J.S. 1981. Genetics of bacterial chemotaxis. *Symp. Soc. Gen. Microbiol.* **31**: 265.
- . 1988. Minireview: Protein phosphorylation in bacterial chemotaxis. *Cell* **53**: 1.
- Purcell, E.M. 1977. Life at low Reynolds number. *Am. J. Phys.* **45**: 3.
- Ravid, S., P. Matsumura, and M. Eisenbach. 1986. Restoration of flagellar clockwise rotation in bacterial envelopes by insertion of the chemotaxis protein, CheY. *Proc. Natl. Acad. Sci.* **83**: 7157.
- Russo, A.F. and D.E. Koshland, Jr. 1983. Separation of signal transduction and adaptation functions of the aspartate receptor in bacterial sensing. *Science* **220**: 1016.
- Segall, J.E., S.M. Block, and H.C. Berg. 1986. Temporal comparisons in bacterial chemotaxis. *Proc. Natl. Acad. Sci.* **83**: 8987.
- Segall, J.E., A. Ishihara, and H.C. Berg. 1985. Chemotactic signaling in filamentous cells of *Escherichia coli*. *J. Bacteriol.* **161**: 51.
- Segall, J.E., M.D. Manson, and H.C. Berg. 1982. Signal processing times in bacterial chemotaxis. *Nature* **296**: 855.
- Shioi, J., C.V. Dang, and B.L. Taylor. 1987. Oxygen as attractant and repellent in bacterial chemotaxis. *J. Bacteriol.* **169**: 3118.
- Silverman, M. and M. Simon. 1974. Flagellar rotation and the mechanism of bacterial motility. *Nature* **249**: 73.
- Spudich, J.L. and D.E. Koshland, Jr. 1975. Quantitation of the sensory response in bacterial chemotaxis. *Proc. Natl. Acad. Sci.* **72**: 710.
- Stewart, R.C. and F.W. Dahlquist. 1987. Molecular components of bacterial chemotaxis. *Chem. Rev.* **87**: 997.
- Stock, A., T. Chen, D. Welsh, and J. Stock. 1988. CheA protein, a central regulator of bacterial chemotaxis, belongs to a family of proteins that control gene expression in response to changing environmental conditions. *Proc. Natl. Acad. Sci.* **85**: 1403.
- Vogler, A.P. and J.W. Lengeler. 1987. Indirect role of adenylate cyclase and cyclic AMP in chemotaxis to phosphotransferase system carbohydrates in *Escherichia coli* K-12. *J. Bacteriol.* **169**: 593.
- Wolfe, A.J., M.P. Conley, and H.C. Berg. 1988. Acetyladenylate plays a role in controlling the direction of flagellar rotation. *Proc. Natl. Acad. Sci.* (in press).
- Wolfe, A.J., M.P. Conley, T.J. Kramer, and H.C. Berg. 1987. Reconstitution of signaling in bacterial chemotaxis. *J. Bacteriol.* **169**: 1878.
- Wylie, D., A. Stock, C.-Y. Wong, and J. Stock. 1988. Sensory transduction in bacterial chemotaxis involves phosphotransfer between Che proteins. *Biochem. Biophys. Res. Commun.* **151**: 891.